Relative Computed Tomography (CT) Enhancement Value for the Assessment of Microvascular Architecture in Renal Cell Carcinoma

Authors' Contribution:
Study Design A
Data Collection B
Statistical Analysis C
Data Interpretation D
Manuscript Preparation E
Literature Search F
Funds Collection G

BE 1 Ai-mei Ouyang
C 1 Zhao-long Wei
D 1 Xin-you Su
F 1 Kun Li
E 2 Dong Zhao
AG 3 De-xin Yu
AG 3 Xiang-xing Ma

1 Medical Imaging Center, Jinan Central Hospital, Shandong University, Jinan, Shandong, P.R. China
2 Department of Pathology, Jinan Central Hospital, Shandong University, Jinan, Shandong, P.R. China
3 Department of Radiology, Qilu Hospital of Shandong University, Jinan, Shandong, P.R. China

Corresponding Authors: Xiang-xing Ma, e-mail: xiangxingma2006@163.com, De-xin Yu, e-mail: ydx0330@sina.com
Source of support: This work was supported by The Fundamental Research Funds of Shandong University (No. 2014QLKY01)

Background: To investigate the correlation between the relative computed tomography (CT) enhancement value and the microvascular architecture in different pathologic subtypes of renal cell carcinoma (RCC).

Material/Methods: This retrospective study included 55 patients with pathologically confirmed RCC. Immunohistochemistry for CD34 was performed for all surgical specimens. Microvascular architecture parameters (density, area, diameter, and perimeter) for the microvessels and the microvessels with lumen were determined. The CT scan was performed during arterial phase or venous phase. The correlation of parameters on CT and tumor angiogenesis was investigated.

Results: Density of microvessels showed a positive correlation with CT values of tumors, ratios of tumor to cortex, and differences of tumor and medulla, but no correlation with CT value ratio of tumor to aorta or tumor to medulla. CT parameters were positively correlated with microvascular parameters. However, no CT parameter differences between hypo-vascular clear cell RCC and papillary RCC was observed. Strikingly, the density and area of the microvessels were significantly higher in hypo-vascular clear cell RCC than that in papillary RCC, while the density of the microvessels with lumen in the cyst-present RCC was significantly higher than that in the cyst-absent RCC. The values (especially those of microvessels with lumen) of area density, diameter, and perimeter were higher in the capsule-absent RCC than in the capsule-present RCC.

Conclusions: The relative CT enhancement value of RCC was associated with vascular architecture parameters including density, area, and perimeter. Quantitative and semi-quantitative parameters on enhanced CT may shed some light on tumor vasculature and function as indicators of the biological behavior of RCC.

MeSH Keywords: Angiogenesis Inducing Agents • Carcinoma, Renal Cell • Four-Dimensional Computed Tomography • Immunohistochemistry

Abbreviations: **CT** – computed tomography; **RCC** – renal cell carcinoma; **MVD** – microvessel density; **S** – area; **D** – diameter; **L** – perimeter; **VTA** – the CT value of tumor during arterial phase; **RTA** – the CT value ratio of tumor to aorta; **RTC** – the CT value ratio of tumor to cortex; **RTM** – the CT value ratio of tumor to medulla; **DTC** – the CT value difference of tumor and cortex; **DTM** – the CT value difference of tumor and medulla; **DAV** – the CT value difference of tumor in arterial and venous phases; **ccRCC** – clear cell renal cell carcinoma; **pRCC** – papillary renal cell carcinoma; **ROI** – region of interest.

Full-text PDF: https://www.medscimonit.com/abstract/index/idArt/902957

📄 2754   🗏 5   📊 2   📖 28

Background

Renal cell carcinoma (RCC) accounts for 3% of all adult malignancies and an estimated 116,000 people worldwide die of this disease annually [1]. Of the subtypes of RCC, clear cell RCC (ccRCC) is the most common [2]. On enhanced computed tomography (CT) scans, the appearance of ccRCC has been described as rapid wash-in and wash-out [3]. Its enhancement varies greatly and some manifest as hypo-vascular on enhanced CT imaging [4,5], which is similar to papillary RCC (pRCC). However, the enhancement mechanism of ccRCC remains unclear.

Angiogenesis plays an important role in tumor invasion and metastasis [6–8]. The gold standard for the measurement of tumor angiogenesis currently is microvessel density (MVD), which has a relationship with tumor growth, metastasis, and prognosis that has been confirmed [9–11]. Both MVD and vascular architecture can affect the biological behavior of the tumor [12,13]. It has been reported that anti-angiogenesis drugs mainly target intratumoral immature vessels instead of mature ones [14]. The maturity of vessels is reflected in the morphology of the microvessels, especially vessels with lumen [15]. Therefore, a comprehensive assessment on tumor angiogenesis requires the combination of MVD and other vascular architecture parameters. The microvascular architecture of the liver has been well-studied [16]. However, there are few studies on microvascular architecture in RCC. MVD has several substantial limitations. For example, it is a kind of invasive, *in vitro* and non-functional measurement and requires precision of tissue preparation. Hence it may not be an ideal indicator for evaluating tumor angiogenesis.

Perfusion CT is a promising imaging technique to quantify tumor angiogenesis because of its noninvasive nature. However, its long scan duration and high radiation dose are persistent problems [7,17]. As a simple, noninvasive and widely-used imaging modality, enhanced CT scan is reliable in RCC examinations, and can, to some extent, display the hemodynamics of the tumor *in vivo* [18]. Nonetheless, the correlation of parameters on enhanced CT and the microvascular architecture of

tumor have been rarely discussed. In the current study, the correlation of enhanced CT parameters with microvascular architecture of the tumor was investigated and the performance of enhanced CT on assessing RCC angiogenesis was studied. It was expected that enhanced CT could provide more detailed information on the diagnosis, treatment, and prognosis of RCC through evaluating angiogenesis.

Material and Methods

Patients

From October 2012 to December 2015, 55 patients (31 males and 24 females, with ages ranging from 28 to 70 years, mean age 55.5 years) with pathologically confirmed RCC were enrolled in this study. Of the 55 cases, there were 44 cases of ccRCC, seven cases of papillary RCC (pRCC), three cases of chromophobe RCC (cRCC) and one case of undifferentiated RCC. There were 31 cases of RCCs found in the left kidneys while 24 cases were confirmed in the right side. The diameter of RCCs varied from 1.3 cm to 9.5 cm. The basic patient information is listed in Table 1. No patient had received preoperative radiotherapy or chemotherapy. The few cases of chromophobe and unclassified RCC were excluded from the statistical analysis. This study was approved by the Institutional Review Board of Qilu Hospital of Shandong University.

CT scanning

CT scanning was performed with a 64-slice CT scanner (GE Discovery CT750, General Electric, Waukesha, WI, USA) during breath-hold. Using a high pressure syringe, 60–80 mL (1.2 mL/kg) of nonionic contrast agent (Omnipaque, 300 mg iodine/mL; GE Healthcare, Shanghai, China) was intravenously administered through the antebrachial vein at a flow rate of 3–5 mL/second. Scanning for the arterial (corticomedullary) phase was started 30 seconds after contrast injection. The venous (nephrographic) phase began 80 seconds after contrast administration. All images were acquired by using a 140-kVp tube voltage and 260–280-mA tube current.

Table 1. Clinical characteristics of the 55 patients.

Patients (n=55)	Age (yr)	Gender		Location		Diameter (cm)
		Female	Male	Right	Left	
Clear cell RCC (n=44)	28–68	18	26	21	23	1.3–9.5
Papillary RCC (n=7)	43–70	3	4	5	2	2.9–5.0
Chromophobe RCC (n=3)	39–67	1	2	0	3	4.4–8.4
Undifferentiated RCC (n=1)	66	0	1	0	1	1.1

RCC – renal cell carcinoma.

CT image analysis

CT images were transferred to a PACS workstation (IMPAX 6.3.1.4095, Agfa Healthcare NV, Belgium) and two experienced radiologists performed the image analysis and measurements collaboratively. The region of interest (ROI) was chosen so that it would be large enough to avoid volume effect. Four ROIs were placed at different sites in the marginal region while two ROIs were placed differently in the center of the lesion. Necrotic areas and vessels within the tumor were avoided. The mean values were measured and recorded.

The following CT findings were analyzed in our study: 1) subgroups assigned according to the CT findings including tumor cyst, necrosis, and pseudo-capsule; 2) the CT value of the tumor in artery phase (VTA, HU); 3) the CT value ratio of tumor/aorta in arterial phase (RTA); 4) the CT value ratio of tumor/cortex in arterial phase (RTC); 5) the CT value ratio of tumor/medulla in arterial phase (RTM); 6) the CT value difference of tumor and renal cortex in arterial phase (DTC, HU); 7) the CT value difference of tumor and renal medulla in arterial phase (DTM, HU); 8) the CT value difference of tumor in artery phase and venous phase (DAV, HU).

Immunohistochemistry

It was ensured that the site of tissue sampling corresponded with the ROI selected. Specimens were fixed in 10% neutral formalin, paraffin-embedded and sliced into 4 μm serial sections. Tissue sections were stained using mouse anti-human monoclonal CD34 antibody and goat anti-mouse polyclonal antibody (Fuzhou Maxim Biotechnology Co. Ltd., Fuzhou, China) using the streptavidin-peroxidase method, following the instructions provided by the company.

Determination of microvessel density (MVD)

MVD was determined as described by Weidner [19]. Single endothelial cell or cells in bundles were counted, while the vessels with a diameter greater than eight erythrocytes or thick muscular walls, and those in the sclerotic region were excluded. Microvessels was defined as CD34-positive single endothelial cell or cell clusters which were distinct from the surrounding tumor cells and connective tissue. Vessels with punctiform, fissured, circular or irregular lumens were defined as microvessels with lumen. The total area (S), diameter (D), and perimeter (L) occupied by positive endothelial cells and lacuna bounded by them were quantified with pixels.

Four random fields from the periphery of the section and two fields from the center were selected under high magnification (200×). The following parameters were measured using an image analyzer system (Image plus 6.0, Media Cybernetics Inc.,

Rockville, MD, USA): MVD (MVD1), area (S1), diameter (D1), and perimeter (L1) of the microvessels and those (MVD2, S2, D2, and L2) of the microvessels with lumen.

Statistical analysis

Data were analyzed using statistical software (SAS, version 9.2; SAS Institute Inc., Cary, NC, USA). Results were expressed as mean ± standard errors. After normality test, a student's t-test was performed to compare between groups. One-way ANOVA was used for comparing multiple groups. After global testing, Student-Newman-Keuls (SNK) post hoc test was performed for post hoc analysis. Pearson's correlation coefficient (r) was used to investigate the relationships between the microvascular architectonic and parameters on CT. A p value less than 0.05 was considered statistically significant.

Results

RCC enhancement on CT

Of the 44 ccRCCs, cysts were present in 14 cases and pseudo-capsules were present in 12 cases while 35 carcinomas displayed heterogeneous enhancement and nine appeared homogeneous. In the seven pRCCs, there were three with cysts, one with pseudo-capsule, heterogeneous enhancement in four, and homogeneous in three.

Correlation of microvascular parameters with parameters on CT in 44 ccRCCs

The mean MVD1, S1, D1, L1, MVD2, S2, D2, and L2 in the 44 ccRCCs were: 17.99±1.55; 66,883.99±6,049.52; 1,560.96±237.58; 6,960.99±629.24; 12.88±1.26; 50,360.96±4,725.43; 847.39±75.46; and 3,535.95±323.37, respectively. Student's t-test showed MVD2, S2, D2, and L2 of the microvessels with lumen were significantly less than those (MVD1, S1, D1, and L1) of the microvessels (p<0.05 for each comparison) (Figure 1A). The mean VTA, DTC, DTM, DAV, RTA, RTC, and RTM in the 44 ccRCCs were: 114.30±17.23; 27.70±4.18; 52.79±7.96; 15.73±2.37; 0.47±0.07; 0.80.0±0.12; and 1.926±0.29, respectively (Figure 1B).

CcRCC were hyper-vascular tumor and strongly enhanced with a CT value close to that of renal cortex during arterial phase.

Student's t-test was performed to analyze the parameters of the microvessels and the microvessels with lumen between the cyst-present and cyst-absent groups, and between the capsule-present and capsule-absent groups in the 44 cRCCs (Table 2). MVD2 was significantly higher in the cyst-present group (n=14) than the cyst-absent group (n=30; t=2.10, p=0.043). There
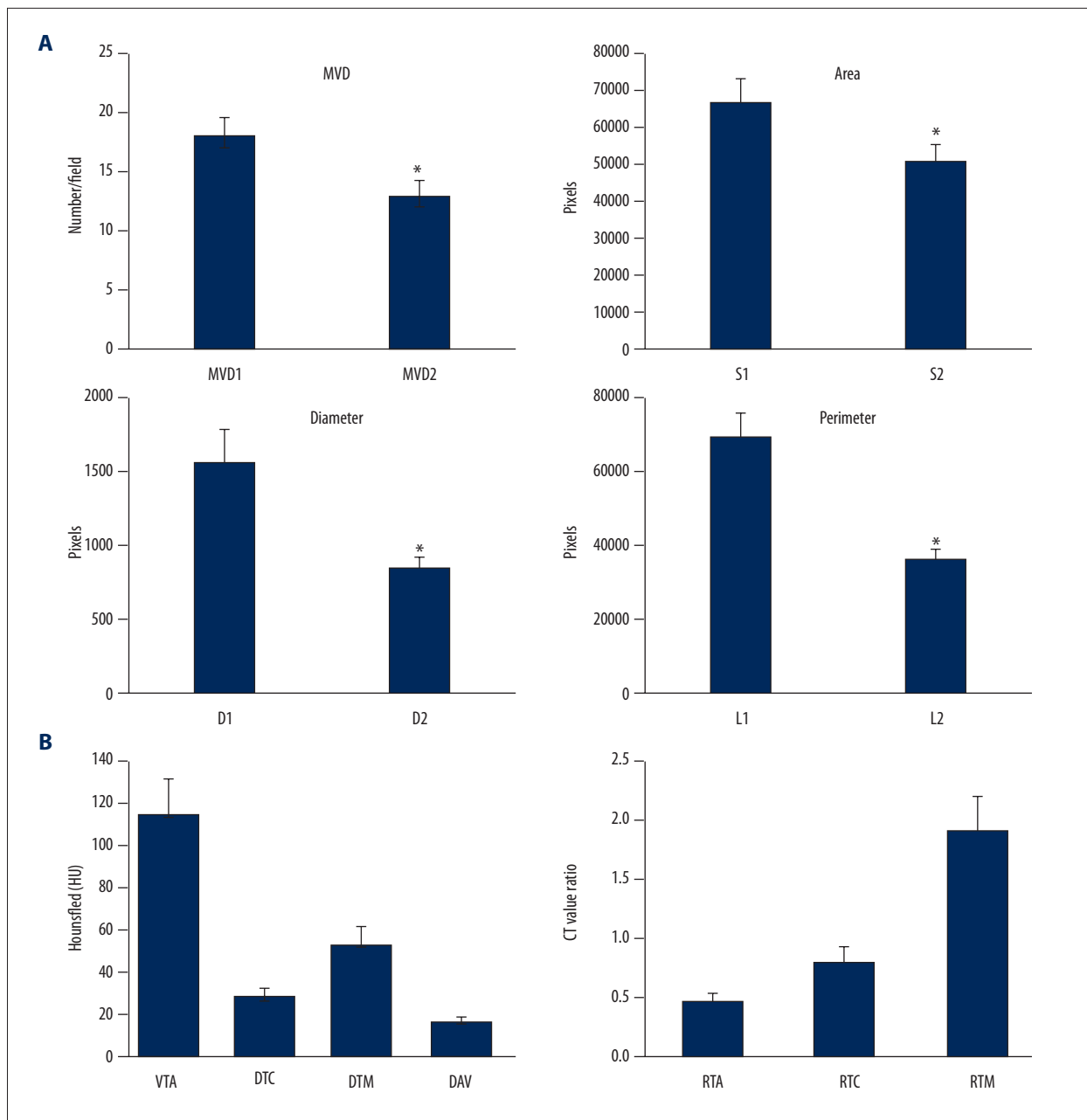
Figure 1. Comparison of microvascular parameters and measurements of parameters on CT in 44 ccRCCs. (**A**) Comparison of microvascular parameters including MVD, areas, diameters, and perimeters between the microvessels and the microvessels with lumen in 44 ccRCCs. MVD2, S2, D2, and L2 of the microvessels with lumen were all significantly less than those of the microvessels (MVD1, S1, D1, and L1) (* $p<0.05$ for each comparison). (**B**) Measurements of parameters on CT in 44 ccRCCs.

was no significant difference with regard to MVD1, S1, D1, L1, S2, D2, and L2 between the cyst-present and the cyst-absent groups ($p>0.05$). The capsule-present group showed a significant higher value of S1, MVD2, S2, D2, and L2 than the capsule-absent group ($p<0.05$) whereas no significant difference was found in other parameters ($p>0.05$).

Pearson's correlation coefficient (r) was used to determine the correlation of vascular parameters and parameters on CT (Table 3). MVD1 was positively correlated with VTA, RTC, DTC, and DTM (r=0.47, 0.36, 0.33, 0.44, respectively; $p<0.05$ for all), but was not correlated with RTA or RTM (r=0.30 and 0.34, respectively; $p>0.05$ for both; Table 4).

Table 2. Comparisons of vascular architecture parameters between subgroups according to the presence of cyst and pseudocapsule in 44 ccRCCs on CT.

	Cyst-present (n=14)	Cyst-absent (n=30)	T	P	Capsule-present (n=12)	Capsule-absent (n=32)	T	P
	Mean ±SE	Mean ±SE			Mean ±SE	Mean ±SE		
MVD1	21.94±2.90	18.83±1.34	0.76	0.452	2.43±2.45	22.04±1.82	0.62	0.543
S1	83559.10±10304.12	73129.50±6415.88	0.72	0.481	61012.67±5685.75	89828.33±7218.20	−2.07	0.049
D1	1529.80±202.45	1473.18±85.90	0.22	0.824	1452.29±127.42	1535.78±130.05	−0.32	0.750
L1	8277.60±1351.99	7439.12±432.72	0.55	0.586	7963.08±839.92	7845.20±112.89	0.17	0.943
MVD2	15.44±2.26	10.03±1.34	2.10	0.043	10.10±1.24	16.17±1.41	−2.26	0.032
S2	62932.19±7657.04	54766.87±5559.94	0.70	0.488	35704.20±5741.47	73825.66±4281.76	−4.17	<0.001
D2	1043.88±131.01	928.79±82.01	0.62	0.541	700.71±103.72	1172.08±77.72	−2.84	0.009
L2	4358.09±625.95	822.17±307.89	0.66	0.516	2787.20±407.62	4938.01±347.72	−3.00	0.006

T indicates *t* value.

Table 3. Correlation of vascular architecture parameters and parameters on CT in ccRCC (n=44).

		VTA	RTA	RTC	RTM	DTC	DTM	DAV
MVD1	r	0.47**	0.30	0.36**	0.34	0.33**	0.44**	0.33
	P	0.005	0.091	0.039	0.055	0.050	0.011	0.062
S1	r	0.47**	0.41**	0.51**	0.44**	0.50**	0.48**	0.42**
	P	0.005	0.017	0.002	0.010	0.003	0.004	0.014
D1	r	0.01	0.08	0.06	−0.06	0.14	−0.02	0.04
	P	0.987	0.655	0.718	0.744	0.439	0.911	0.847
L1	r	0.38**	0.36**	0.42**	0.22	0.41**	0.33	0.27
	P	0.031	0.038	0.015	0.221	0.018	0.059	0.126
MVD2	r	0.72**	0.56**	0.59**	0.51**	0.56**	0.66**	0.58**
	P	<0.001	<0.001	<0.001	<0.001	<0.001	<0.001	<0.001
S2	r	0.69**	0.51**	0.64**	0.59**	0.63**	0.66**	0.60**
	P	<0.001	0.002	<0.001	<0.001	<0.001	<0.001	<0.001
D2	r	0.81**	0.61**	0.71**	0.62**	0.69**	0.75**	0.65**
	P	<0.001	<0.001	<0.001	<0.001	<0.001	<0.001	<0.001
L2	r	0.81**	0.59**	0.68**	0.63**	0.68**	0.76**	0.70**
	P	<0.001	<0.001	<0.001	<0.001	<0.001	<0.001	<0.001

** Indicates a statistical significance.

VTA increased as MVD did, suggestive of a higher enhancement of tumor during arterial phase (Figure 2). RTC and DTM tended to be higher as MVD increased. Correlation was noted between S1 and measurements including VTA, RTA, RTC, RTM, DTC, DTM and DAV with a higher correlation coefficient than other microvascular parameters, suggesting that tumor enhancement degree was associated with the area of microvascular perfusion. VTA and RTC showed positive correlations with MVD1, S1, and L1, respectively. Whereas RTM had single correlation with S1, as DAV did. Furthermore, correlations

Table 4. Relationships of MVD1 and MVD2 in groups with different values of RTC (n=44).

	RTC ≤0.6 (n=7)	0.6< RTC <1 (n=23)	RTC ≥1 (n=14)	F	P
MVD1	16.52±3.24*	19.04±0.03	24.90±2.44	7.98	<0.01
MVD2	6.88±1.43*	12.33±1.47#	20.38±2.07	18.62	<0.001

* Indicates a significant difference between the subgroup of RTC ≤0.6 and the other subgroups; # represents a significant difference between the subgroup of 0.6< RTC <1 and the subgroup of RTC ≥1.
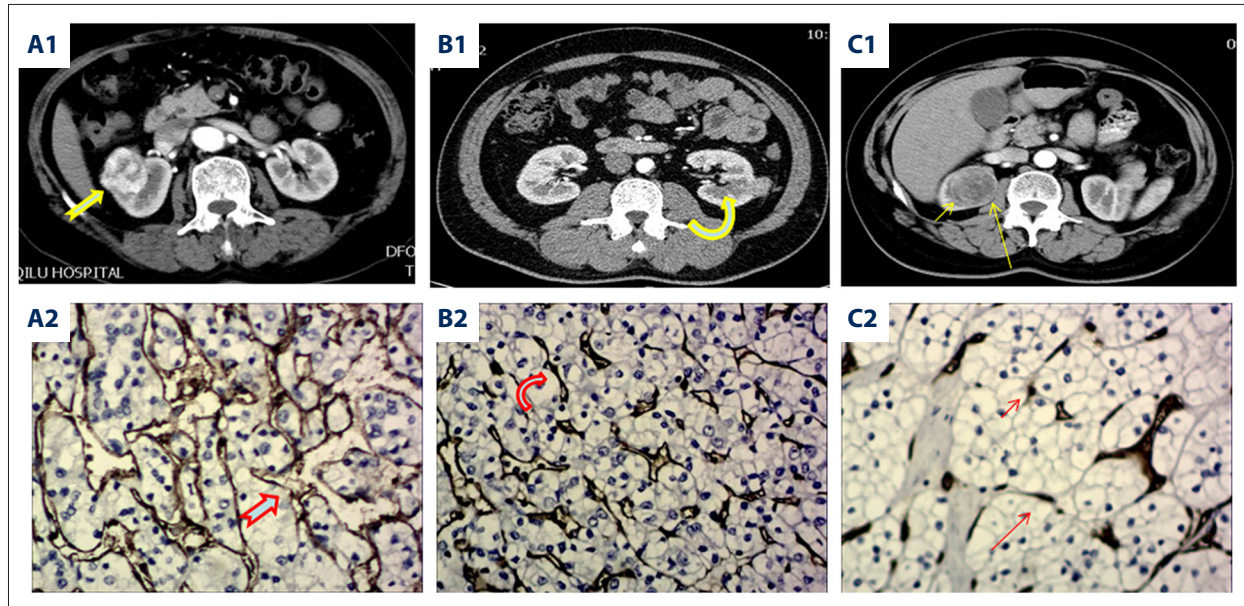

Figure 2. CT scan and immunohistochemical staining results (CD34, 200×) of three cases. (**A1, A2**, a 67-year-old woman): Obvious heterogeneous contrast enhancement in the right kidney (bold arrow) with a VTA value of 160 HU and a RTV value of 1.3 was displayed. There were many microvessels which mainly consisted of relatively mature vessels with lumen (bold arrow) and the microvascular areas were the largest. (**B1, B2**, a 44-year-old man): Moderate homogeneous contrast enhancement in the left kidney (curved arrow) with a VTA value of 87 HU and a RTV value of 0.75 was displayed. Microvessels mainly consisted of vessels with fissured lumen (curved arrow) and the microvascular area was large. (**C1, C2**, a 59-year-old man): Mild contrast enhancement (long arrow) with a VTA value of 80 HU and a RTC value of 0.6 was displayed. Pseudo-capsule (short arrow) appeared as hyper density in the lesion margin. There were a few microvessels which involvement in microvessels without lumen mostly (long and short arrows) and the microvascular area was the smallest.

were noted between DTM with MVD1 and S1. MVD2, S2, D2, and L2 exhibited positive correlations with parameters on CT during the arterial phase. VTA had stronger correlation with the parameters of the microvessels with lumen (MVD2, S2, D2, and L2; r=0.72, 0.69, 0.81, and 0.81, respectively; $p<0.001$) than those of the microvessels (MVD1, S1, and L1; $p<0.05$). These results indicate that parameters including VTA, RTA, RTC, RTM, DTC, DTM, and DAV tended to increase with the rise of MVD2, S2, D2, and L2.

Compared with RTM, RTC showed a stronger correlation with microvascular parameters (MVD1 and S1). In terms of parameters of the microvessels with lumen (MVD2, S2, D2, and L2), both RTM and RTC displayed highly correlations. In the present study, tumor enhancement on CT was decided by the vessel areas, especially that of the microvessels with lumen.

Collectively, these results suggested that tumor parameters on enhanced CT can reflect the growth of microvessels to some extent.

Comparison of hyper-vascular with hypo-vascular ccRCCs

The 44 ccRCCs were categorized into three groups according to the RTC value, which included groups of RTC ≤0.6, 0.6< RTC <1, and RTC ≥1. The one-way ANOVA with post hoc SNK's comparisons was used for multiple groups. The mean MVD1 in the groups of RTC ≤0.6, 0.6< RTC <1, and RTC ≥1 were 16.52±3.24, 19.04±0.03, and 24.90±2.44, respectively (Table 4). Significant difference was noted in MVD1 in the group of RTC ≤0.6 with the other groups (F=7.98, $p<0.01$), while MVD1 did not differ significantly from the groups of 0.6< RTC <1 and RTC ≥1. The mean MVD2 in the groups of RTC ≤0.6, 0.6 <RTC <1, and RTC

Table 5. Comparisons of microvascular architecture parameters and parameters on CT between pRCC (n=7) and hypovascular ccRCC (n=7).

		pRCC (n=7)	Hypovascular ccRCC (n=7)	T	P
		Mean ±SE	Mean ±SE		
Microvessel	MVD1	6.98±0.91	16.52±3.24	−2.84	0.015
	S1	22827.39±3999.84	69526.38±15637.62	−2.89	0.013
	D1	1772.40±1283.19	1287.90±252.13	0.37	0.718
	L1	3507.88±1119.63	6189.04±1270.97	−1.58	0.139
Microvessel with lumen	MVD2	4.81±0.50	6.88±1.43	−1.37	0.212
	S2	7664.88±3901.69	30420.19±9186.08	−1.28	0.225
	D2	314.70±40.16	479.67±108.48	−1.43	0.179
	L2	1400.59±230.26	2043.80±395.04	−1.41	0.185
Parameters on CT	VTA	58.71±4.91	71.29±3.47	−2.09	0.059
	VTV	67.57±5.58	73.43±4.72	−0.80	0.439
	RTA	0.31±0.05	0.32±0.03	−0.31	0.762
	RTC	0.47±0.05	0.54±0.02	−1.29	0.220
	RTM	0.98±0.12	1.26±0.15	−1.47	0.168
	DTC	−72.29±13.34	−61.43±3.72	−0.78	0.448
	DTM	−5.00±7.77	11.86±6.45	−1.67	0.121
	VAV	−8.86±4.00	−1.43±4.94	−1.17	0.265

≥1 were 6.88±1.43, 12.33±1.47, and 20.38±2.07, respectively, with significant difference between each other (F=18.62, $p<0.001$). If RTC ≤0.6 was defined as the cutoff value of hyper-vascular and hypo-vascular tumors, there were seven hypo-vascular carcinomas in the 44 ccRCCs.

Parameters on enhanced CT in pRCC

Seven pRCCs demonstrated hypodense enhancement on arterial phase with a mean VTA of 58.71±4.91 (range 42~85 HU). The mean RTA, RTC, and RTM were 0.31±0.05, 0.47±0.05, and 0.98±0.12, respectively, while the mean DTC, DTM, and DAV were −72.29±13.34, −5.00±7.77, and −8.86±4.00, respectively, with RTC less than 0.6.

Correlation of vascular parameters with parameters on CT in hypo-vascular ccRCCs and pRCCs

The RTC was less than 0.6 in the seven hypo-vascular ccRCCs and seven pRCCs. Student's *t*-test between the two groups found that the vascular parameters were generally higher in hypo-vascular ccRCCs than in the pRCCs with significant difference in MVD1 and S1 and no difference in D1, L1, MVD2, S2, D2, and L2 (Table 5). Meanwhile, parameters on CT, including

VTA, VTV, RTA, RTC, RTM, DTC, DTM, and VAV, did not differ significantly between the two groups. It can be deduced that hypo-vascular ccRCC has a similar enhancement pattern but quite a different mechanism in pRCC. There were more microvessels in hypo-vascular ccRCC with fewer microvessels with lumen, which provided effective perfusion. However, there were fewer microvessels in pRCC with more microvessels with lumen, showing similar perfusion status of ccRCC.

Discussion

RCC is a typical angiogenesis-dependent tumor in which angiogenesis is closely associated with tumor growth, metastasis, and prognosis [6]. Spiral multi-phasic enhanced CT scanning can display multi-phasic imaging of the kidney through a single intravenous injection of contrast media, thus providing information on diagnosis, treatment, and prognosis of RCC [20]. It has become an imaging method widely used in clinical practice. Previous studies [20,21] on spiral enhanced CT scanning of RCC are mostly limited to research on CT value, which could be affected by the dose, administration rate, and concentration of the contrast agents, and on the scan delay time as well as the circulation, renal function, and weight

and body surface area of the patient. Therefore, it cannot be used to perform comprehensive assessment on tumor vascularity. The application of relative CT value can provide more information on tumor vascularity as it can screen the influence of intrinsic and extrinsic factors [22]. Enhancement degree of the tumor on CT has been shown to correlate significantly with MVD [23].

MVD is the parameter most frequently used to quantify intra-tumoral angiogenesis [11]. Tumor angiogenesis is a complex process where single endothelial cells, strip-like or fork-like endothelial cells bud, and mature microvessels with lumen can be found [15,23]. In the present study, vascular parameters, including MVD, area, diameter, and perimeter of the microvessels and the microvessels with lumen were studied as these architecture parameters play a role in the biological behavior of tumor through influencing blood supply [24–26]. All vascular parameters were correlated with CT parameters during arterial phase with a higher correlation in the microvessels than in the microvessels with lumen. Moreover, the vascular area had a stronger correlation with parameters on CT than MVD. Vascular perimeter was correlated with RTA, RTC, and DTC, although the correlation was weaker than that of the area. This suggests that, besides MVD, microvascular architecture also plays an important role in tumor perfusion.

Positive correlations were found between MVD with VTA, RTC, and DTC in RCC while no relationship was found between MVD with RTM. This may be attributed to ccRCC having a higher incidence in the renal cortex and hyper-vascular region. Therefore, RTC and DTC make better indicators for tumor perfusion. MVD was not correlated with RTA and RTM, due to possible individual difference in delay time. The CT value of the aorta declines slower than RCC during the period between arterial and venous phases, while the CT value of the medulla has a faster increase as scan time extends.

It has been shown that ccRCC has a high likelihood of hyaline changes, fibrosis, and coagulative necrosis [23]. In the current study of ccRCC, 31.8% (n=14) had cysts and 27.2% [13] had pseudo-capsules, presenting a disagreement with prior reports [27,28]. In the cyst-present ccRCCs, the mean parameters of the microvessels and the microvessels with lumen were higher than cyst-absent ccRCCs with significant difference in MVD2. The mean S1, MVD2, S2, D2, and L2 in the capsule-absent ccRCCs were significantly higher than capsule-present ccRCCs. But no significant difference was observed in MVD1 between the two groups. The presence of cyst and absence of capsule are indicative of malignancy, and tumors tend to grow faster and be more aggressive, which results in tumors outgrowing the blood supply from the microvessels with lumen and undergoing cystic changes from necrosis. On enhanced CT, ccRCC can also be hypo-vascular with a similar enhancement degree to pRCC and a different mechanism from pRCC.

Conclusions

The enhancement of RCC on CT was associated with vascular architecture parameters including MVD (especially that of the microvessels with lumen), area, and perimeter. Thus, quantitative and semi-quantitative parameters of RCC on spiral enhanced CT imaging can shed some light on the tumor vascularity and function as the indicators of the biological behavior of RCC. One study limitation was that the study concentrated on ccRCC and pRCC and did not investigate the correlations in other subtypes. Further studies on the correlations between microvascular architecture parameters and parameters on enhanced CT in other subtypes are warranted.

Ethics approval

This study was approved by the Institutional Review Board of Qilu Hospital of Shandong University.

Competing interests

All authors declare that they have no competing interests.

References:

1. Ljungberg B, Campbell SC, Choi HY et al: The epidemiology of renal cell carcinoma. Eur Urol, 2011; 60: 615–21

2. Neely BA, Wilkins CE, Marlow LA et al: Proteotranscriptomic analysis reveals stage specific changes in the molecular landscape of clear-cell renal cell carcinoma. PloS One, 2016; 11: e0154074

3. Muglia VF, Prando A: Renal cell carcinoma: Histological classification and correlation with imaging findings. Radiol Bras, 2015; 48: 166–74

4. Wu PY, Lin SF, Wu PH et al: Multiple hypovascular tumors in kidney: A rare case report and differential diagnosis. Case Rep Med, 2013; 2013: 595193

5. Onishi T, Oishi Y, Goto H et al: Histological features of hypovascular or avascular renal cell carcinoma: The experience at four university hospitals. Int J Clin Oncol, 2002; 7: 159–64

6. Folkman J, Beckner K. Angiogenesis imaging. Acad Radiol, 2000; 7: 783–85

7. Das CJ, Thingujam U, Panda A, Sharma S, Gupta AK: Perfusion computed tomography in renal cell carcinoma. World J Radiol, 2015; 7: 170–19

8. Iagaru A, Gambhir SS: Imaging tumor angiogenesis: The road to clinical utility. Am J Roentgenol, 2013; 201: W183–91

9. Brekken RA, Thorpe PE: Vascular endothelial growth factor and vascular targeting of solid tumors. Anticancer Res, 2001; 21: 4221–29

10. Zhang JP, Yuan HX, Kong WT et al: Increased expression of Chitinase 3-like 1 and microvessel density predicts metastasis and poor prognosis in clear cell renal cell carcinoma. Tumor Biol, 2014; 35: 12131–37

11. Kouhsoltani M, Halimi M, Dibazar S: A positive correlation between immunohistochemical expression of CD31 and mast cell tryptase in odontogenic tumors. Pol J Pathol, 2015; 66: 170–75

12. Sharma S, Sharma MC, Gupta DK, Sarkar C: Angiogenic patterns and their quantitation in high grade astrocytic tumors. Neurooncol, 2006; 79: 19–30

13. Khadim MT, Ahmed SA, Khan FA et al: Evaluation of vascular endothelial growth factors A, C and D as indicators of lymphangiogenesis and angiogenesis in invasive and non-invasive urothelial carcinoma bladder. J Pak Med Assoc, 2015; 65: 851–56

14. Vasudev NS, Reynolds AR: Anti-angiogenic therapy for cancer: Current progress, unresolved questions and future directions. Angiogenesis, 2014; 17: 471–94.

15. Kan Z, Phongkitkarun S, Kobayashi S et al: Functionnal CT for quantifying tumor perfusion in antiangiogenic therapy in a rat model. Radiology, 2005; 237: 151–58

16. Yu DX, Cai YH, Ma XX: Angiogenesis and maturation of hepatocellular carcinoma. Journal of Shandong University (Health Sciences), 2009; 6: 51–54

17. Xie Q, Wu J, Tang Y et al: Whole-organ CT perfusion of the pancreas: Impact of iterative reconstruction on image quality, perfusion parameters and radiation dose in 256-slice CT-preliminary findings. PLoS One, 2013; 8: e80468

18. Wu T, Li RF, Lu SH: The contrastive study of parameters of CT contrast agent in the kidney enhancement scanning. Journal of Gannan Medical University, 2013; 33: 14–28

19. Weidne N: Tumour vascularity and proliferation: Clear evidence of a close ralationship. Pathol, 1999; 189: 297–99

20. Tsili AC, Argyropoulou MI: Advances of multidetector computed tomography in the characterization and staging of renal cell carcinoma. World J Radiol, 2015; 7: 110–27

21. Kim JK, Kim TK, Ahn HJ et al: Differentiation of subtypes of renal cell carcinoma on helical CT scans. Am J Roentgenol, 2002; 178: 1499–506

22. Zhang J, Lefkowitz RA, Ishill NM et al: Solid renal cortical tumors: Differentiation with CT. Radiology, 2007; 244: 494–504

23. Yang Y, Zhou JL, Guo L: [A correlative study between CT features and the expression of Ki67 and MVD,P73 in clear renal cell carcinoma.] Chinese Journal of CT and MRI, 2005; 13: 51–54 [in Chinese]

24. Sharma SG, Aggarwal N, Gupta SD et al: Angiogenesis in renal cell carcinoma: Correlation of microvessel density and microvessel area with other prognostic factors. Int Urol Nephrol, 2011; 43: 125–29

25. Sullivan CA, Ghosh S, Ocal IT et al: Microvessel area using automated image analysis is reproducible and is associated with prognosis in breast cancer. Hum Pathol, 2009; 40: 156–65

26. Ehling J, Theek B, Gremse F et al: Micro-CT imaging of tumor angiogenesis: Quantitative measures describing micromorphology and vascularization. Am J Pathol, 2014; 184: 431–41

27. Teng J, Gao Y, Chen M et al: Prognostic value of clinical and pathological factors for surgically treated localized clear cell renal cell carcinoma. Chin Med J (Engl), 2014; 127: 1640–44

28. Roquero L, Kryvenko ON, Gupta NS, Lee MW: Characterization of fibromuscular pseudocapsule in renal cell carcinoma. Int J Surg Pathol, 2015; 23: 359–63